Two-port reflective grating with the cancellation of the zeroth order

CHEN FU, BO WANG*, JIMIN FANG, KUNHUA WEN, ZIMING MENG, QU WANG, ZHAOGANG NIE, XIANGJUN XING, LI CHEN, LIANG LEI, JINYUN ZHOU
School of Physics and Optoelectronic Engineering, Guangdong University of Technology, Guangzhou 510006, China

In this paper, a two-port reflective grating with the cancellation of the zeroth order is introduced. The grating uses an Ag reflective metal grating structure. Under a normal incidence of light with a wavelength of 1550 nm, for both TE and TM polarizations, the grating can output in ±1st orders. In addition, the efficiency of the 0th order reflected light is less than 1%. Optimized grating parameters are obtained by using rigorous coupled-wave analysis. Furthermore, the complex physical mechanism of multimode superposition coupling in grating can be well explained by modal method.

(Received November 14, 2019; accepted August 18, 2020)

Keywords: Two-port splitting, Reflective grating, Beam splitter, Cancellation of the zeroth order

1. Introduction

A beam splitter is an important optical device which is widely used in various fields [1-5]. It can be applied in optical path switches [6-8], laser resonators [9-11], the picosecond optical signal processing [12-15], photonic integrated circuits [16,17], and quantum key distribution systems [18]. Feng et al. designed a two-port single-layer dielectric grating beam splitter with polarization independent at a Bragg angle of incidence [19]. Wang et al. designed a low-contrast grating with cancellation of the zeroth order [20] and a mixed metal dielectric grating with suppression of the zeroth order [21]. Yin et al. [22] designed an encapsulated metal-dielectric reflective grating which presented for broadband polarization-independent two-port beam splitting under normal incidence at the central wavelength of 800 nm. The results indicated that a bandwidth of 46.4 nm could be achieved for the diffraction efficiency over 46% at the central wavelength of 800 nm. Sang et al. [23] found out the asymmetrical lateral leakage of light in a finite zero-contrast grating mirror and proposed the dispersion equation of slab waveguide for the TM mode to evaluate the resonant condition of the zero-contrast grating mirror. The results show that the mirror effect of the infinite zero-contrast grating is resulted from the overlapping of order-mode resonance pairs. Sang et al. [24] studied tunable optical reflectance using a monolithic encapsulated grating in fused silica grating based on the guided-mode resonance effect. And they found that the thickness of top layer controlled the guided-mode resonance location, and the thickness of the grating layer controlled the leakage of the energy to the substrate thus controlled the surface reflectivity. A polarization-independent two-port grating with the cancellation of the zeroth order at normal incidence is designed in this paper. The grating structure is a single-layer fused-silica grating with a connecting layer. Compared with reported Ref. [20], the grating structure of this paper adds a layer of Ag reflective material to change the transmission-type grating into a reflection-type grating. In addition, compared to reported Ref. [21], the grating incorporates a connecting layer of fused silica. The rigorous coupled-wave method [25], the modal method [26] and the finite-difference time-domain method [27] are basic theories of analyzing gratings.

In this paper, a two-port reflection grating beam splitter with good beam splitting effect is designed by using rigorous coupled-wave analysis method. Then the modal method is used to obtain the effective refractive index of each mode of the grating region, and the energy distribution of the grating diffraction process can be observed. Based on the grating structure parameters calculated by rigorous coupled-wave analysis method, the efficiency of the ±1st order under TE polarization reaches 48.01%, the efficiency of the ±1st order under TM polarization reaches 47.90%. Analyzing the incident characteristics and process tolerances of the grating with the zeroth order being cancelled, the diffraction efficiency of the ±1st order under two polarizations can exceed 47% within a suitable bandwidth.

2. Modal analysis and numerical design

The two-port grating is shown in Fig. 1. The grating groove medium is air with the refractive index of n_1=1.00. The grating has an Ag reflective layer with a height of 100 nm and a grating layer of a fused-silica substrate. The groove depth of the grating layer is h_1, and the refractive index of the grating ridge is n_2=1.45. A fused-silica connecting layer is added between the Ag reflective layer and the grating ridge with the connecting layer having a thickness of h_2. The refractive index of the substrate is n_2=1.45. And the duty cycle f of the grating is the ratio of the width of the grating ridge b to the period d. For TE polarization and TM polarization [28], the incident wavelength of the grating is 1550 nm. According to the grating equation [29,30], the period range we chose is between λ and 2λ. After multiple data analysis, the grating period d to 2982 nm and duty cycle f to 0.37 can be set.

As can be seen from Fig. 2, it shows the relationship of the efficiency versus the height h_1 of the grating groove and the thickness h_2 of the connecting layer. For the TE-polarized light with h_1=0.96 μm and h_2=0.17 μm, the efficiency of the 0th order is 0.51% and the efficiency of the ±1st order is 48.01%. The total efficiency of the +1st and the -1st orders is 96.02%. For TM-polarized light, the efficiency of 0th order is 0.85%, and the efficiency of ±1st order is 47.90%. The total efficiency of the two orders is 95.80%. According to the efficiency of each order, it can be seen that the grating shows good performance in reducing the efficiency of 0th order diffraction.

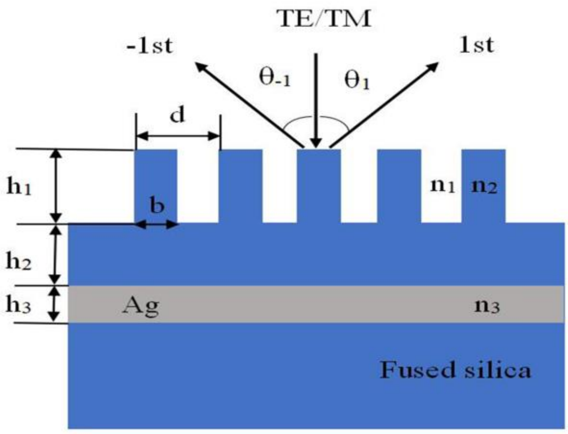

Fig. 1. A two-port reflective grating with the cancellation of the zeroth order

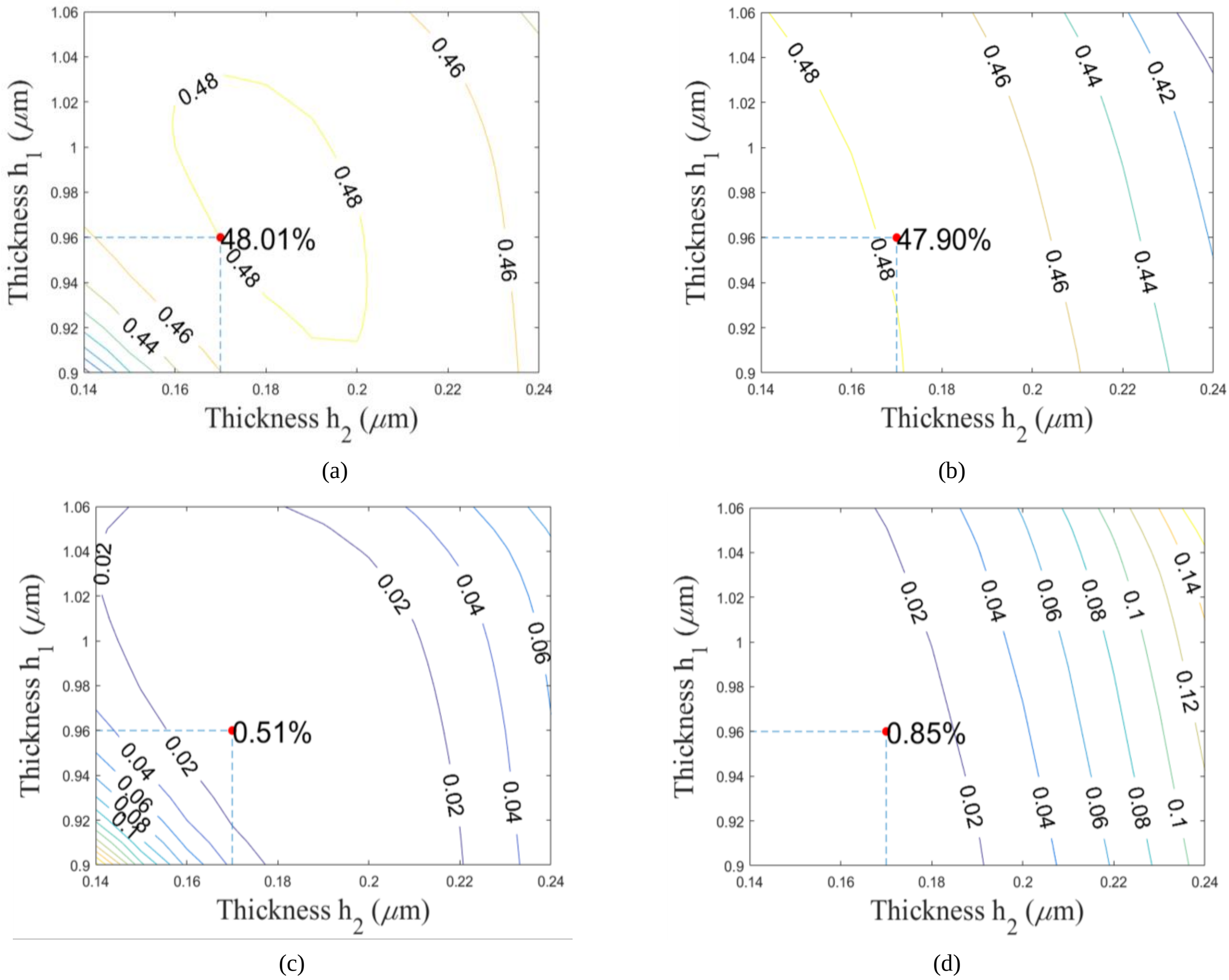

Fig. 2. Efficiencies in two orders for the grating versus the grating groove depth and the thickness of the connecting layer for both two polarizations at wavelength of 1550 nm under normal incidence: (a) the 1st order for TE polarization, (b) the 1st order for TM polarization, (c) the 0th order for TE polarization, (d) the 0th order for TM polarization (color online)

According to the finite-difference time-domain method, Fig. 3 shows the normalized field distribution of the two-port grating. It clearly shows the energy distribution of the upper surface of the grating to the substrate under normal incidence of 1550 nm incident light. Figs. 3(a) and 3(b) depict the splitting effects of TE waves and TM waves, respectively. Since the structure of the grating is periodic, the energy distributed in the grating also exhibits periodic characteristics. TE-polarized light is incident from the top of the grating, and the energy is mostly concentrated at the bottom of the grating ridge and the upper middle section on both sides. The incident light reaches the Ag reflective layer and reflects it out of the grating and is divided into two strands. When TM-polarized light enters the grating, the energy is concentrated at the bottom of the grating ridge. And then after reflection, it is divided into 1st order and -1st order at the top of the grating ridge.

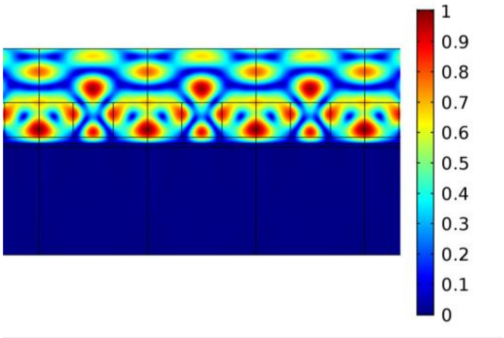

(a)

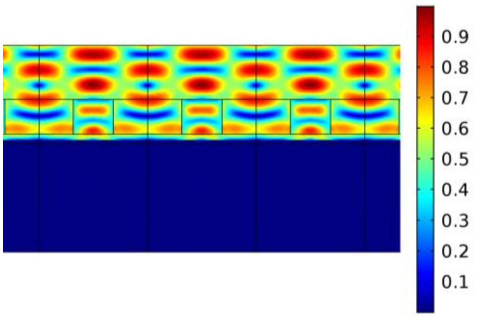

(b)

Fig. 3. Normalized field magnitude distribution with the two-port beam splitter under normal incidence: (a) TE polarization, (b) TM polarization (color online)

The rigorous coupled-wave method can only provide the diffraction efficiency under the incident of TE-polarized light and TM-polarized light, and the modal method can clearly explain the diffraction process. First, TE-polarized light or TM-polarized light can be coupled to some discrete grating modes, where the coupling efficiency depends on the overlap integral. There are four couplings in the energy exchange inside the grating. For TE polarization, the integral equation is written as:

$$\left\langle E_y^{in}(x) \leftrightarrow u_m(x) \right\rangle = \frac{\left| \int_0^d E_y^{in}(x) u_m(x) dx \right|^2}{\int_0^d \left| E_y^{in}(x) \right|^2 dx \int_0^d \left| u_m(x) \right|^2 dx},$$

and for TM polarization, the integral equation is written as:

$$\left\langle H_y^{in}(x) \leftrightarrow u_q(x) \right\rangle = \frac{\left| \int_0^d H_y^{in}(x) u_q(x) dx \right|^2}{\int_0^d \left| H_y{}^{in}(x) \right|^2 dx \int_0^d \left| u_q(x) \right|^2 dx}.$$

By calculating the overlap integral [31], energy changes from the incident wave to modes 0 and 2 are 0.5364 and 0.4597 for TE polarization or 0.4734 and 0.4005 for TM polarization. Modal method is a detailed analysis and explanation of the physical coupling mechanism of diffracted light waves propagating in reflection and transmission gratings. When the incident light wave enters the ridge of the grating, the first two couplings will occur. At this time, only two grating modes, namely mode 0 and mode 2, are considered. Because other grating modes are excited by evanescent waves, their energy can be ignored. Mode 0 and mode 2 propagate with their different effective refractive indices which can be derived from the eigen equation of the grating. When the modes reach the exit surface of the grating, the last two couplings will occur, which lead to efficiencies in the zeroth and first orders [20].

3. Results and discussion

In the actual manufacturing, the tolerance [32-37] should be found to satisfy needs. For the potential fabrication process, the silver, fused-silica, chromium photoresist layers can be coated on the substrate. After lithography, photoresist grating can be formed, which can be transferred to the chromium layer to form a mask. By inductively coupled plasma etching, the connecting -layer-based grating with a metal layer can be fabricated. Fig. 4 shows the relationship between the two orders of the two-port reflective grating beam splitter and the grating period. The abscissa is the period of the grating, and the ordinate is the efficiency of each order. It can be seen from the Fig. 4 that for TE polarized light and TM-polarized light, the grating period is in the range of 2965-2990nm, where the reflection efficiencies of the ±1st order are greater than 47%.

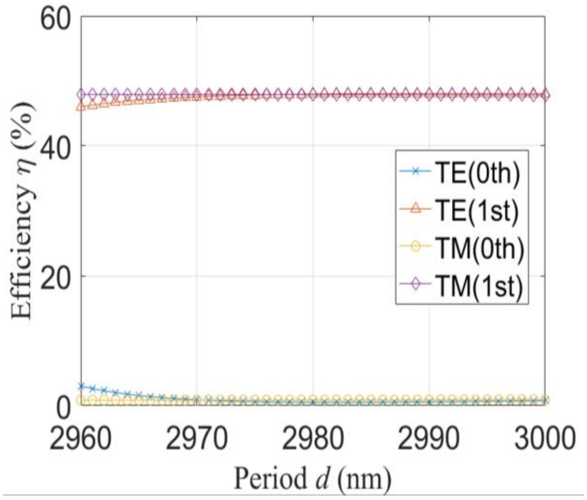

Fig. 4. The efficiency corresponding to the period at wavelength of 1550 nm with duty cycle of 0.37 under normal incidence (color online)

At the same time, the change of the incident wavelength will also affect the beam splitting effect of the grating. Fig. 5 shows the relationship between the reflection efficiency of a two-port grating and the incident wavelength. The abscissa indicates the incident wavelength and the ordinate indicates the reflection efficiency. It can be seen from the Fig. 5 that for TE-polarized light, the incident wavelength is in the range of 1530 to 1550 nm, and the efficiency of 1st order is greater than 47%, where the efficiency of 0th order is less than 1%. For TM-polarized light, the incident wavelength is in the range of 1525 to 1560nm, and the efficiency of ±1st order is greater than 47%, where the efficiency of 0th order is less than 2%.

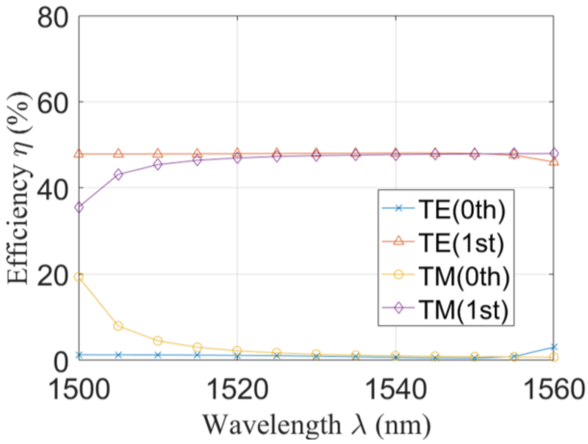

Fig. 5. The efficiency corresponding to the incident wavelength with duty cycle of 0.37 under normal incidence (color online)

Fig. 6 shows the relationship between transmission efficiency and duty cycle of the grating under two polarizations. When the duty cycle varies between 0.37 and 0.40, efficiencies of ±1st order for TE- and TM-polarized lights exceed 47%. In this range of duty cycle, the two-port splitting effect of the two-port reflective grating under TE polarization and TM polarization is substantially equal.

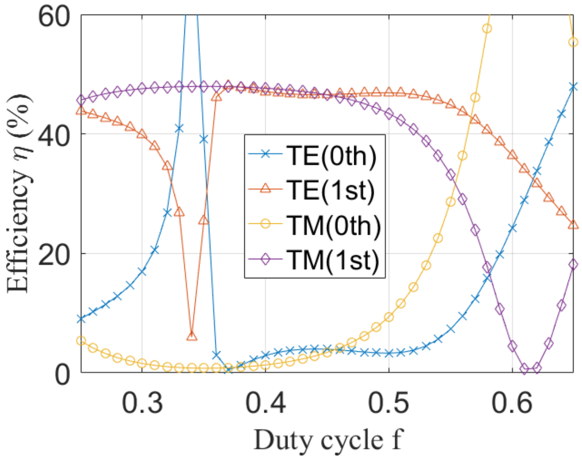

Fig. 6. The diffraction efficiency corresponding to the duty cycle at wavelength of 1550 nm under normal incidence (color online)

In this paper, the incident angle condition of the grating is normal incidence. The tolerance of the incident angle also needs to be taken into consideration, which is shown in Fig. 7. In two polarizations, there is a sudden change in the efficiency of these four orders in the range of from -3° to -1° and from 1° to 3°. In the remaining range, the change in efficiency is relatively stable. In the range of from -0.1° to 0.3°, the 1st order under TE polarization exceeds 47%. In the range of from -1.3° to 0.7°, the 1st order under TM polarization exceeds 47%.

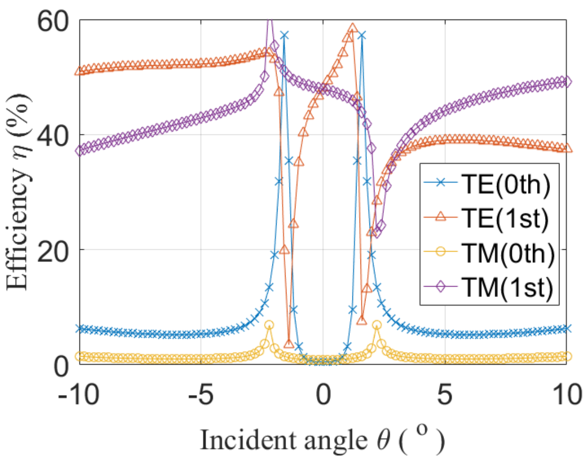

Fig. 7. The diffraction efficiency corresponding to the incident angle at wavelength of 1550 nm under normal incidence (color online)

4. Conclusion

In this paper, we have designed a two-port grating beam splitter with the cancellation of the zeroth order. Though analyzing and calculating the structural parameters of the grating by the rigorous coupled-wave theory. For TE-polarization light, efficiencies of the ±1st orders are both 48.01%, and the efficiency of the 0th order is 0.51%. For the TM-polarization light, efficiencies of the ±1st orders are both 47.90%, where the efficiency of the 0th order is 0.85%. It can be seen from the results that the grating has a good suppression effect on the 0th order. This kind of zeroth-order suppressed grating is useful in many optical systems. At the same time, by analyzing, the results show good incident bandwidth and period tolerance under both TE-polarized and TM-polarized light incidence.

Acknowledgements

This work is supported by the Science and Technology Program of Guangzhou (202002030284, 202007010001).

References

[1] P. Mahalakshmi, P. K. Choudhury, M. S. Mani. Rajan, M. Sharma, R. Maheswar, Optik **185**, 1295 (2019).
[2] Y. Xia, H. Zhang, S. Chang, C. Wei, Q. Kuang, L. Hu, Optik **189**, 53 (2019).
[3] H. Haroon, A. Kareem, Optoelectron. Adv. Mat. **13**(5), 290 (2019).
[4] M. Singh, Optik **178**, 902 (2019).
[5] C.-P. Wei, Z.-M. Wu, C.-Z. Deng, L.-Y. Hu, Opt. Commun. **452**, 189 (2019).
[6] A. Gharaati, N. Miri, Optoelectron. Adv. Mat. **11**(11), 608 (2017).
[7] J. Wang, J. Miao, P. Xu, S. Zhang, Y. Duan, Opt. Commun. **454**, 124378 (2020).
[8] X. Xing, H. Liu, W. Shang, Z. Chen, Opt. Commun. **451**, 28 (2019).
[9] Y. Wang, Y. Chen, B. Zhang, D. Liu, Z. Xu, Z. Li, X. Cai, Y. Sang, P. Wang, J. Guo, W. Liu, Opt. Commun. **451**, 35 (2019).
[10] J. Zhao, H. Li, H. Gu, X. Diao, Opt. Commun. **453**, 124375 (2019).
[11] M. Kim, Optik **176**, 523 (2019).
[12] J. Li, Y. Tang, Z. Kuang, J. Schille, U. Loeschner, W. Perrie, D. Liu, G. Dearden, S. Edardson, Opt. Laser Eng. **112**, 59 (2019).
[13] A. Cominelli, G. Acconcia, M. Ghioni, I. Rech, Opt. Eng. **57**(3), 031302 (2018).
[14] V. N. Lednev, S. M. Pershin, P. A. Sdvizhenskii, M. Y. Grishin, M. A. Davydov, A. Y. Stavertiy, R. S. Tretyakov, Laser Phys. Lett. **14**(2), 026002 (2017).
[15] M. Shen, S. Liu, W. Zhao, H. Qi, G. Peng, Opt. Laser Technol. **105**, 52 (2018).
[16] Y. Wang, D. Zhang, S. Xu, B. Xu, Z. Dong, T. Huang, Optoelectron. Adv. Mat. **12**(5), 283 (2018).
[17] E. Rafiee, F. Emami, R. Negahdari, Optik **172,** 234 (2018).
[18] Y.-Y. Fei, X.-D. Meng, M. Gao, Z. Ma, H. Wang, Optik **170**, 368 (2018).
[19] J. Feng, C. Zhou, J. Zheng, H. Cao, P. Lv, Appl. Opt. **48**(29), 5636 (2009).
[20] B. Wang, Sci. Rep. **5**, 16501 (2015).
[21] B. Wang, IEEE Photon. J. **8**(1), 7801706 (2016).
[22] Z. Yin, Y. Lu, J. Yu, C. Zhou, Chin. Opt. Lett. **18**(7), 070501 (2020).
[23] T. Sang, X. Yin, H. Qi, J. Gao, X. Niu, H. Jiao, IEEE Photon. J. **12**(2), 4500111 (2020).
[24] T. Sang, G. Chen, Y. Wang, B. Wang, W. Jiang, T. Zhao, S. Cai, Opt. Laser Technol. **83**, 163 (2016).
[25] M. G. Moharam, D. A. Pommet, E. B. Grann, T. K. Gaylord, J. Opt. Soc. Am. A **12**(5), 1077 (1995).
[26] I. C. Botten, M. S. Craig, R. C. Mcphedran, J. L. Adams, J. R. Andrewartha, Opt. Acta **28**(3), 413(1981).
[27] Y. Xu, F. Wang, Y. Gao, W. Chen, C. Chen, X. Wang, Y. Yi, X. Sun, D. Zhang, Opt. Commun. **463**, 125418 (2020).
[28] Z. Xu, T. Lyu, X. Sun, Opt. Commun. **451**, 17 (2019).
[29] F. Zhang, Z. Zhang, D. Gao, X. Wang, IEEE T. Electron. Dev. **66**(9), 4022 (2019).
[30] X. Gao, T. Ning, C. Zhang, J. Xu, J. Zheng, H. Li, J. Li, L. Pei, H. You, Opt. Commun. **454**, 124441 (2020).
[31] A. Panda, P. Sarkar, G. Palai, Optik **157**, 944 (2018).
[32] H. Li, B. Wang, Opt. Eng. **55**(9), 097109 (2016).
[33] C. Xiang, C. Zhou, W. Jia, J. Wu, Chin. Opt. Lett. **16**(7), 070501 (2018).
[34] L. Qian, W. Zhu, K. Wang, C. Yan, Opt. Commun. **443**, 123 (2019).
[35] C. Gao, B. Wang, K. Wen, Z. Meng, Z. Nie, X. Xing, L. Chen, L. Lei, J. Zhou, Opt. Commun. **452**, 395 (2019).
[36] J. Xiao, J. Liu, J. Han, Y. Wang, Opt. Commun. **452**, 411 (2019).
[37] S. Sahu, J. Ali, G. Singh, Opt. Appl. **48**(1), 161 (2018).

*Corresponding author: wangb_wsx@yeah.net